Supporting Information for 'Ultrafast Spectroscopic Observation of a Quantum Chain Reaction: The Photodecarbonylation of Solid Diphenylcyclopropenone'

by Stephanie C. Doan, Gregory Kuzmanich, Matthew N. Gard, Miguel A. Garcia-Garibay and Benjamin J. Schwartz

Dept. Chem. & Biochem., UCLA, Los Angeles, CA 90095-1569

1 Solution-Phase Experiments on DPCP and DPA

For our experiments studying the photodecarbonylation of DPCP in solution, we prepared samples of both DPCP and DPA in cyclohexane and circulated these samples through a spectrophotometer flow cell. Our initial experiments used a 266-nm excitation wavelength and a broad-band probe, the results of which are shown in Figure 1. The data show that other than a slight broadening at early times in the DPCP sample (right panel), there is no significant difference in the transient absorption dynamics between DPCP and DPA. We strongly suspected that this similarity between the two samples resulted from the very strong absorption cross section of DPA and an inability to clear the flow cell of the photoproduct in an efficient manner.

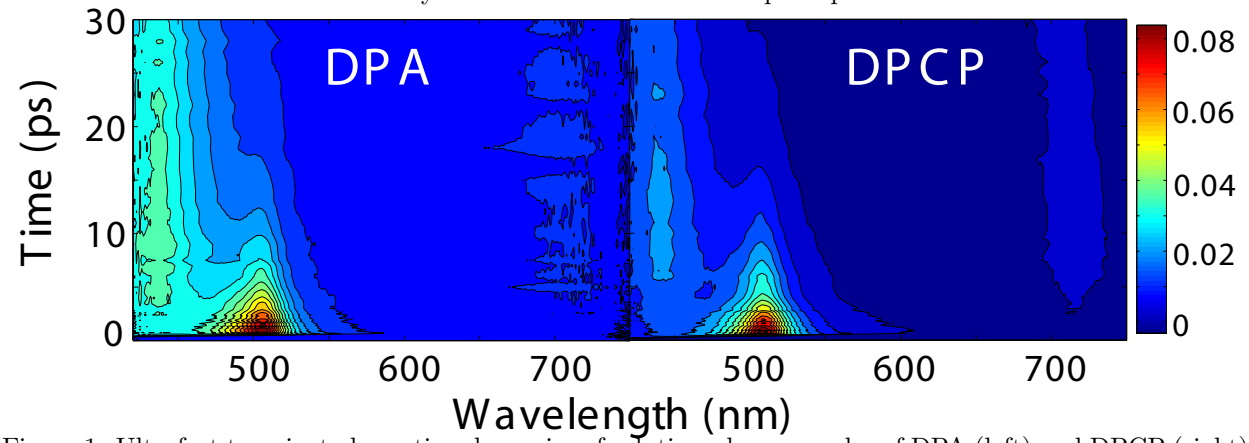

Figure 1: Ultrafast transient absorption dynamics of solution-phase samples of DPA (left) and DPCP (right) in cyclohexane following excitation at 266 nm. Color bar values are given in Δ OD.

To investigate whether or not this was the case, we changed the excitation wavelength to 310 nm, where DPCP still absorbs strongly but the DPA photoproduct has minimal absorption. The transient absorption spectral dynamics that resulted from exciting at this wavelength is shown in Figure 2. The data show a strong absorption at ∼480 nm that decays in about 200 fs, which can be attributed to S_2-DPCP*, as previously assigned by Takeushi and Tahara.[1] We note that although the absorption cross section of DPA is small at this excitation wavelength, it is not completely negligible, as trace absorption of the S_2-DPA* (∼500 nm) and S_1-DPA* (∼450 nm) can be seen in the data at later times. Single-time slices of this data spectra at 0, 1 and 5 ps are (normalized and) presented in the first figure of the main paper.

2 Preparation of DPCP and DPA Nanocrystalline Suspensions

2.1 General Methods

Chemicals of the highest available purity were purchased from Sigma-Aldrich. Chromatographic purification was accomplished with Silica-P flash silica gel (40–62 ∘A) purchased from SiliCycle Inc.

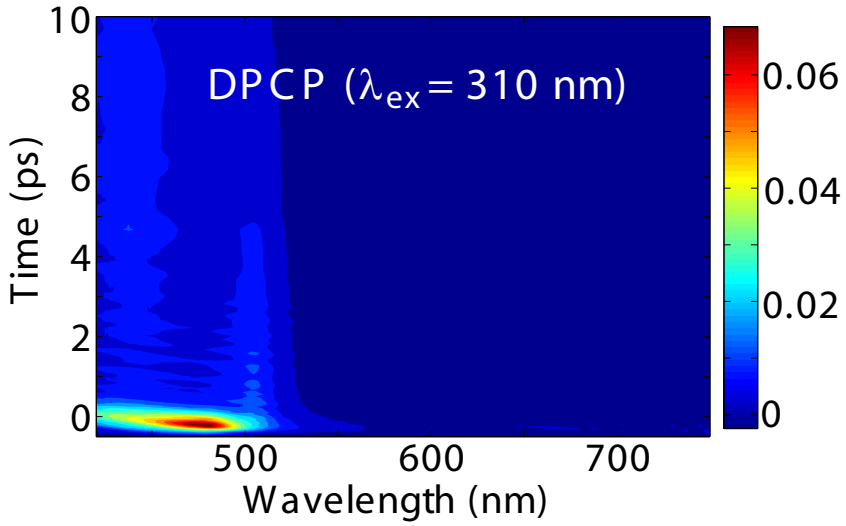

Figure 2: Ultrafast transient absorption dynamics of solution-phase DPCP in cyclohexane following excitation at 310 nm. Color bar values are given in Δ OD.

2.2 Purification of Diphenylcyclopropenone (DPCP) and Diphenylacetylene (DPA)

Commercially available DPCP (98%) was purified by column chromatography through a silica gel column using methylene chloride as the eluent and subsequently twice recrystallized by slow solvent evaporation in the dark from cyclohexane to give pure white prisms. Commercially available DPA was recrystallized by slow solvent evaporation from cyclohexane to give pure white flakes.

2.3 Preparation of Nanocrystalline Suspensions

All nanocrystalline suspensions were prepared either under low intensity illumination or under red light. Nanocrystalline suspensions for microscopy, dynamic light scattering (DLS) studies, and transient absorption spectroscopy were prepared by injecting 2-μL of a DPCP (0.1 M) solution in acetone into 5-mL of vortexing water (Millipore).[2, 3] The resulting suspension ($4x10^{-5}$ M) was sonicated three times at room temperature for 4 min, allowing for 2 min rest between runs. These samples were not made using surfactant.

For the ultrafast measurements, approximately one liter of nanocrystalline suspension was created for each experiment. It was found that if one liter of suspension was made at once, lower quality nanocrystals were observed, which would precipitate more quickly. Approximately 200, 5-mL aliquots of nanocrystals were created in individual 10-mL testtubes. These 5-mL aliquots were then combined in a large 2-L round bottom flask, which was subjected to reduced pressure for one hour to ensure complete removal of any residual acetone. DPCP nanocrystals obtained in this manner were characterized using DLS, atomic force microscopy (AFM), and scanning electron microscopy (SEM).[3] These studies revealed prisms in the range of ∼50-200 nm consistent with those described in references [2] and [3]. Powder X-ray diffraction of filtered nanocrystals confirmed the anhydrous form of DPCP with the space group Pbcn.[4]

3 Experimental Apparatus for Ultrafast Pump-Probe Spectroscopy

The ultrafast laser pulses used in our experiments were derived from an Ti:Sapphire amplifier (Coherent, Legend Elite) seeded with a broadband Ti:Sapphire oscillator (Coherent, Mantis). The output of the amplifier (35 fs, 3.2 mJ at 800 nm, 1-kHz repetition rate) was split with into two beams with roughly equivalent power.

The 266-nm excitation pulses were generated using one of these two beams in a "double-mixing" scheme in which part of the beam is split off and doubled in a BBO crystal, with the resultant 400-nm light combined with the remaining 800 nm light in a second BBO crystal cut for sum-frequency generation. For the solution experiments, the 310-nm pump light was created by sending the other half of the originally-split 800-nm amplified output beam through an optical parametric amplifier (Light Conversion, TOPAS) that was tuned to produce 620-nm light. This 620-nm beam was then doubled in a BBO crystal to create 310-nm light pulses. The broadband probe pulse for all the experiments was created by splitting off a small amount of the 800-nm beam prior to the mixing stage using a quartz flat at near-normal incidence. This low-intensity beam was then focused into a sapphire plate to create visible white-light continuum probe pulses. Data acquisition was accomplished using a commercially-built spectrometer (HELIOS, Ultrafast Systems LLC).

4 2DCoA of the DPCP and DPA Transient Absorption Data

Similar to the time-domain double Fourier transform methods used extensively for multi-pulse NMR experiments, generalized two dimensional correlation analysis (2DCoA) utilizes a simple cross-correlation analysis with any perturbation-induced spectral intensity change as a function of two independent variables, wavelength and time in our case, over a specified interval of time. A 2D correlation spectrum is better able to resolve overlapping bands by spreading a normal 1D spectrum over a second dimension. To accomplish this, one must use a *dynamic spectrum*, $\tilde{y}(\nu, t)$, defined as:[5, 6, 7, 8]

$$\tilde{y}(\nu,t) = \begin{cases} y(\nu,t) - \bar{y}(\nu) & \text{for } T_{\min} \leq t \leq T_{\max} \\ 0 & \text{otherwise} \end{cases} \tag{1}$$

in which $y(\nu, t)$ represents the experimentally measured, perturbed spectra in a chosen time window ($T_{\min} \leq t \leq T_{\max}$) and $\bar{y}(\nu)$ is the *reference spectrum*, often chosen to be[5, 6, 7, 8]

$$\bar{y}(\nu) = \frac{1}{T_{\max} - T_{\min}} \int_{T_{\min}}^{T_{\max}} y(\nu,t)\,\mathrm{d}t \tag{2}$$

the average of the measured spectra over the chosen time range. With this dynamic spectrum, a 2D correlation spectrum can be constructed via[5, 6, 7, 8]

$$\mathrm{X}(\nu_1,\nu_2) = \langle \tilde{y}(\nu_1,t) \cdot \tilde{y}(\nu_2,t') \rangle, \tag{3}$$

where the angle brackets represent a cross correlation. This correlation spectrum $\mathrm{X}(\nu_1, \nu_2)$ provides a measure of the relative similarity and dissimilarity in the evolving 1D spectrum. A typical analysis begins by separating a 2D correlation spectrum into its real and imaginary parts[5, 6, 7, 8]

$$\mathrm{X}(\nu_1,\nu_2) = \Phi(\nu_1,\nu_2) + i\Psi(\nu_1,\nu_2) \tag{4}$$

in which $\Phi(\nu_1, \nu_2)$, the *synchronous* 2D correlation intensity, shows spectral correlations that are similar, or which happen in phase. In contrast, $\Psi(\nu_1, \nu_2)$, the *asynchronous* 2D correlation intensity, contains information on the dissimilar, or out of phase, evolution of the perturbed spectrum.[5, 6, 7, 8]

If $y(\nu, t)$ were a continuous function $\Phi(\nu_1, \nu_2)$ and $\Psi(\nu_1, \nu_2)$ could be easily determined using Fourier transforms. In practical application, however, spectral data is obtained as a discrete set of points that can be represented as a matrix:[8]

$$\tilde{\mathbf{y}}(\nu) = \begin{bmatrix} \tilde{y}(\nu,t_1) \\ \tilde{y}(\nu,t_2) \\ \vdots \\ \tilde{y}(\nu,t_m) \end{bmatrix} \tag{5}$$

where it is assumed the reference spectrum, $\bar{y}(\nu)$, has already been subtracted. The synchronous spectrum can then be calculated by taking the inner product of two dynamic spectra matrices,[8]

$$\Phi(\nu_1, \nu_2) = \frac{1}{m-1}\tilde{\mathbf{y}}(\nu_1)^\top \tilde{\mathbf{y}}(\nu_2). \tag{6}$$

The asynchronous spectrum can be obtained from a Hilbert transform,[7, 8]

$$\Psi(\nu_1, \nu_2) = \frac{1}{m-1}\sum_{j=1}^{m} \tilde{y}_j(\nu_1) \cdot \tilde{z}_j(\nu_2), \tag{7}$$

where $\tilde{z}_j(\nu_2)$ represents the discrete orthogonal spectrum, which can obtained from the dynamic spectrum[7, 8]

$$\tilde{z}_j(\nu_2) = \sum_{k=1}^{m} N_{jk} \cdot \tilde{y}_k(\nu_2) \tag{8}$$

in which[7, 8]

$$N_{jk} = \begin{cases} 0 & \text{if } \ j = k \\ 1/\pi(k-j) & \text{otherwise.} \end{cases} \tag{9}$$

When this is applied to a typical data matrix, the result is[8]

$$\Psi(\nu_1, \nu_2) = \frac{1}{m-1}\tilde{\mathbf{y}}(\nu_1)^\top \mathbf{N}\tilde{\mathbf{y}}(\nu_2), \tag{10}$$

where $\mathbf{N}$ is the *Hilbert-Noda transformation matrix*[8]

$$\mathbf{N} = \frac{1}{\pi}\begin{bmatrix} 0 & 1 & \frac{1}{2} & \frac{1}{3} & \dots \\ -1 & 0 & 1 & \frac{1}{2} & \dots \\ -\frac{1}{2} & -1 & 0 & 1 & \dots \\ -\frac{1}{3} & -\frac{1}{2} & -1 & 0 & \dots \\ \vdots & \vdots & \vdots & \vdots & \ddots \end{bmatrix}. \tag{11}$$

Our experimentally collected data utilizes unevenly spaced time points to be able to capture dynamics on multiple time scales with minimal effort. To be able to use such unevenly spaced data, some alterations must be made to the correlation equations. The time-averaged reference spectrum with unevenly spaced points can be represented as[8]

$$\bar{y}(\nu) = \frac{\sum_{j=1}^{m} y_j(\nu) \cdot (t_{j+1} - t_{j-1})}{\sum_{j=1}^{m}(t_{j+1} - t_{j-1})}. \tag{12}$$

To use this method, two points, t_0 and t_{m+1} are defined as[8]

$$t_0 = 2t_1 - t_2 \tag{13}$$

$$t_{m+1} = 2t_m - t_{m-1}. \tag{14}$$

This allows for the calcuation of the synchronous spectrum as[8]

$$\Phi(\nu_1, \nu_2) = \frac{1}{2(t_m - t_1)}\sum_{j=1}^{m} \tilde{y}_j(\nu_1) \cdot \tilde{y}_j(\nu_2) \cdot (t_{j+1} - t_{j-1}) \tag{15}$$

and the asynchronous spectrum as[8]

$$\Psi(\nu_1, \nu_2) = \frac{1}{2(t_m - t_1)}\sum_{j=1}^{m} \tilde{y}_j(\nu_1) \cdot \tilde{z}_j(\nu_2) \cdot (t_{j+1} - t_{j-1}), \tag{16}$$

where the adjusted Hilbert-Noda matrix elements are[8]

$$N_{jk} = \begin{cases} 0 & \text{for } j = k \\ \frac{t_{k+1} - t_{k-1}}{2\pi(t_k - t_j)} & \text{otherwise.} \end{cases} \tag{17}$$

With the above equations for matrices of discrete data at uneven time steps, we used the raw data we measured to construct synchronous and asynchronous transient absorption spectra for both photoexcited DPCP and photoexcited DPA. As discussed in the main text, spreading the 1D spectral data along a second dimension revealed that the broad band on the red side of the spectrum, attributed to DPA, does not stay stationary. In fact, the 2DCoA shows that this band appears to shift as well as broaden. Although this analysis on its own does not provide direct evidence of a quantum chain reaction in the solid-state DPCP system, it does provide much greater insight into the data: for example, the fact that the spectrum shifts and broadens explains why we could not successfully use singular value decomposition to separate the spectrum DPCP* from DPA*. The information about the band positions that we obtained from the synchronous 2D spectra is what provided the starting positions for our Gaussian fits to the original 1D data that are shown in the main text. Overall, until we performed the 2DCoA, we were simply unable to come up with a reasonable model for the DPCP* absorption band to successfully fit and understand our data.

5 Gaussian Fitting

The two-dimensional correlation analysis described above suggests that the DPCP* transient absorption band neither shifts nor changes shape with time. Because of this, we were able to use two Gaussians to fit the S_2-DPCP* band; the two Gaussians had fixed peak centers at 495 nm and 505 nm and fixed band widths of 30 nm and 10 nm, respectively. We also fixed the ratio of the two Gaussian amplitudes at 1:0.6 (495-nm:505-nm) so that only the overall amplitude was allowed to vary with time. As described in the main text, we also fit the transient absorption of DPA produced from decarbonylated solid-state DPCP using two Gaussians to represent the two states elucidated using 2D correlation. We initially constrained these bands to be centered at the positions shown in the 2DCoA, but then allowed the Gaussians to vary in position, amplitude and width in the final fits that we performed. The spectral data from the DPA control sample was also fit with two Gaussians that were allowed to vary in position, amplitude and width.

We also tried an analysis in which we fit the broad DPA* band with a single Gaussian. Although this analysis worked reasonably well for the data on the directly-excited DPA nano crystals, we prefer the two-Gaussian fits for a number of reasons. First, the use of two Gaussians is consistent with the 2DCoA, which shows clearly that broad transient absorption is comprised of two bands. Second, the use of single Gaussian for the DPCP sample is unable to show the spectral changes that we assign to the QCR. This is because most of the spectral changes associated with the QCR occur only at the red edge of experimentally-measured spectrum, and a single Gaussian cannot capture these changes because it must simultaneously fit both the blue and the red edges of the band. Nonetheless, if we proceed and carry out the single-Gaussian fit, we find a significant change in the width of the single Gaussian as well as a significant decrease in the accuracy of the fit over the 2-30 ps window. This means that even with a single Gaussian fit, the DPCP and DPA samples still show different spectral dynamics in the 2-30 ps window. Since neither the one- nor two-Gaussian fits are physically motivated, the different dynamics they show, in combination with the 2DCoA and population analyses described in the text, indicate that all the differences in these samples occur between 2 and 30 ps after excitation, supporting our conclusion that the QCR occurs sequentially rather than concertedly.

Table 1: Gaussian Fitting Parameters for fits represented in Figure 4 of the main paper

	0.75 ps	5 ps	50 ps
DPCP*			
A_1 [a]	$1.48x10^{-2}$	$1.48x10^{-3}$	N/A
DPA*			
A_2 [b]	$3.42x10^{-3}$	$2.86x10^{-2}$	$1.87x10^{-2}$
B_2 [b]	607	657	620
C_2 [b]	40.8	94.1	90.1
A_3 [c]	$5.63x10^{-2}$	$7.53x10^{-2}$	$3.14x10^{-2}$
B_3 [c]	748	1069	757
C_3 [c]	145.2	254.5	100.8
DPA* photo control			
A_4 [d]	$1.79x10^{-3}$	$2.64x10^{-2}$	$2.52x10^{-3}$
B_4 [d]	560	561	562
C_4 [d]	11.6	17.8	19.7
A_5 [e]	$8.46x10^{-2}$	$7.18x10^{-2}$	$5.65x10^{-2}$
B_5 [e]	802	712	696
C_5 [e]	190.5	139.8	130.8

[a] DPCP* Fit (panel a green dot-dash line) = $A_1 * exp^{\frac{-(x-494)^2}{2*10^2}} + (A_1 * 0.6) * exp^{\frac{-(x-505)^2}{2*30^2}}$

[b] DPA* Fit (panel a red dashed line # 1) = $A_2 * exp^{\frac{-(x-B_2)^2}{2*C_2^2}}$

[c] DPA* Fit (panel a red dashed line # 2) = $A_3 * exp^{\frac{-(x-B_3)^2}{2*C_3^2}}$

[d] DPA* Fit (panel b blue dashed line # 1) = $A_4 * exp^{\frac{-(x-B_4)^2}{2*C_4^2}}$

[e] DPA* Fit (panel b blue dashed line # 2) = $A_5 * exp^{\frac{-(x-B_5)^2}{2*C_5^2}}$

References

[1] S. Takeuchi and T. Tahara, "Femtosecond absorption study of photodissociation of diphenylcyclopropenone in solution: Reaction dynamics and coherent nuclear motion," *J. Chem. Phys.*, vol. 120, pp. 4768–4776, 2004.

[2] G. Kuzmanich, A. Natarajan, K. K. Chin, M. Veerman, C. J. Mortko, and M. A. Garcia-Garibay, "Solid-state photodecarbonylation of diphenylcyclopropenone: A quantum chain process made possible by ultrafast energy transfer," *J. Am. Chem. Soc.*, vol. 130, pp. 1140–1141, 2008.

[3] G. Kuzmanich, M. N. Gard, and M. A. Garcia-Garibay, "Photonic amplification by singlet-state quantum chain reaction in the photodecarbonylation of crystalline diarylcyclopropenones," *J. Am. Chem. Soc.*, vol. 131, pp. 11606–11614, 2009.

[4] H. Tsukada, H. Shimanouchi, and Y. Sasada, "X-ray determination of the structure of anydrous diphenylcyclopropenone. variations of the molecular geometry due to hydrogen bonding.," *Chemistry Letters*, vol. 3, pp. 639–642, 1974.

[5] I. Noda, "Generalized two-dimensional correlation method applicable to infrared, raman, and other types of spectroscopy," *Appl. Spectrosc.*, vol. 47, pp. 1329–1336, 1993.

[6] I. Noda, "Generalized two-dimensional correlation spectroscopy," *Appl. Spectrosc.*, vol. 54, pp. 236A–248A, 2000.

[7] I. Noda, "Determination of two-dimensional correlation spectra using the hilbert transform," *Appl. Spectrosc.*, vol. 54, pp. 994–999, 2000.

[8] I. Noda and Y. Ozaki, *Two-Dimensional Correlation Spectroscopy – Applications in Vibrational and Optical Spectroscopy.* John Wiley & Sons, Ltd, 2004.